Noncontact measurement metho high-frequency impedance of l wire harness

著者（英）	Tomohiro Yoshikawa, Jianqing Wang, Yasunori Oguri, Makoto Tanaka, Michihira Iida
journal or publication title	IEEE Transactions on Electromagnetic Compatibility
volume	61
number	1
page range	271-278
year	2019-02
URL	http://id.nii.ac.jp/1476/00006564/

doi: 10.1109/TEMC.2018.2805318(http://doi.org/10.1109/TEMC.2018.2805318)

Non-Contact Measurement Method for High-Frequency Impedance of Load at the End of Wire Harness

Tomohiro Yoshikawa, Jianqing Wang, *Member, IEEE,* Yasunori Oguri, Makoto Tanaka, and Michihira Iida

***Abstract*—Request to non-contact measurement method of load impedance connected to a wire harness is increasing rapidly. A method using network analyzer together with two current probes were previously proposed for this purpose, but it is valid only to 20 ∼30 MHz. In this study, we extended the above-mentioned non-contact measurement method to FM band by applying transmission line theory to the wire harness. The validity of the newly proposed measurement method was confirmed experimentally, and as a result the load impedance was measured with an error within 10% up to 100 MHz.**

***Index Terms*—Wire harness, load impedance, non-contact measurement, transmission line.**

I. Introduction

In recent years, the vehicle system itself for controlling a car has been shifting from a group of independent individual controls such as engine control, brake control, air conditioner control to the integrated control in which a plurality of control systems cooperate to realize a complex function. The increase in the number of electronic devices mounted to control a car is accelerating year by year. Along with that, the noise sources and use of wire harness are also increasing. This will cause noise emission inside and outside the car through the wire harness. In addition, when external noise is induced in a wire harness, there is a possibility of malfunction of the in-vehicle electronic devices. For this reason, the load impedance of electronic equipment connected to wire harness is indispensable for predicting and taking measures against emission characteristics and immunity characteristics, and accurate grasp of the load impedance in circuit design is regarded as important [1]-[3].

Measurement of the load impedance connected to a wire harness can be performed directly by cutting the wire harness. However, it is desirable not to cut the wire harness and measure the impedance during operation of the electronic device. Although a method for measuring load impedance in a non-contact manner in existing research has been reported, it has not been applied to frequencies higher than 30 MHz [4]. Therefore, in this study, we regard the wire harness as a transmission line, propose expansion of the non-contact impedance measurement method to high frequency region using transmission line theory, and verify its validity experimentally. The proposed method allows measuring the impedance of a component connected at the end of two wire harnesses or at the end of a wire harness above a ground plane. A representative component to be measured is the load impedance of motor. The impedance changes when the motor works so that the conducted and radiated noises are time dependent. So non-contact measurement of its load impedance is required. In addition, since the disturbance on in-vehicle FM radios is one of major issues in automobile EMC, we focus the frequency limitation to 100 MHz. This is also because that, when the frequency is higher than 100 MHz, some parasitic components have to be considered in the measuring probes [5] of the non-contact measurement system, which will greatly increase the complexity of the measurement.

The structure of this paper is as follows. Section 2 introduces the conventional non-contact impedance measurement method. In Section 3, the transmission line theory is applied to the wire harness section, and the conventional non-contact measurement method is extended to the high frequency range. Section 4 describes how to derive the characteristic impedance and the propagation speed of the wire harness for applying the transmission line theory. In Section 5, the measurement procedure of the proposed measurement method is summarized, and the experimental verification results are described in Section 6. Section 7 concludes this paper.

II. Non-contact Impedance Measurement Method

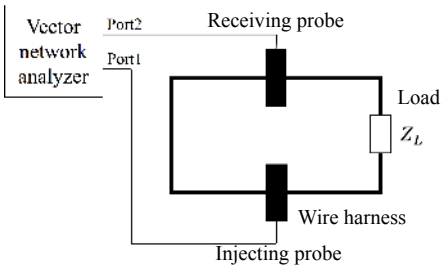

Fig. 1. Non-contact measurement system of load impedance.

Fig. 1 shows a measurement system for non-contact measurement of the impedance Z_L of the load connected to the end of a closed loop of wire harness. The measurement system consists of a current injecting probe, a current receiving probe and a vector network analyzer. A current is applied from Port 1 of the network analyzer to the closed loop of the wire

Manuscript received xx xx, 2017; revised xx xx, 2018.

T. Yoshikawa, and J. Wang are with the Graduate School of Engineering, Nagoya Institute of Technology, Nagoya, 466-8555, Japan (corresponding author e-mail: wang@nitech.ac.jp). Yasunori Oguri, Makoto Tanaka, and Michihira Iida are with DENSO CORPORATION, Japan.

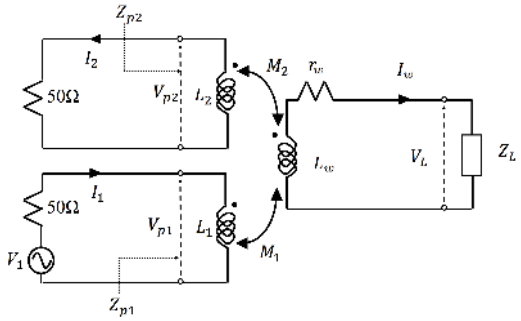

Fig. 2. Equivalent circuit of the measurement system.

harness via the current injectimg probe, and the output of the current receiving probe is measured at Port 2. Fig. 2 shows the equivalent circuit [4] of the measurement system.

In Fig. 2, L_1 and L_2 , V_{p1} and V_{p2} , Z_{p1} and Z_{p2} are the inductance components, induced voltages, input impedances of the current injecting probe and the current receiving probe, respectively. L_w and r_w are the inductance and resistance components of the portion where the current is applied to the wire harness. M_1 and M_2 are the mutual inductances of the current injecting probe and the current receiving probe with respect to the wire harness, respectively. Assuming that the current flowing in the closed loop of the wire harness in the equivalent circuit of Fig. 2 is I_w, we have the following equation:

$$\begin{bmatrix} V_1 \\ 0 \\ -V_L \end{bmatrix} = \begin{bmatrix} 50+Z_{p1} & 0 & -j\omega M_1 \\ 0 & 50+Z_{p2} & j\omega M_2 \\ -j\omega M_1 & j\omega M_2 & r_w+j\omega L_w \end{bmatrix} \begin{bmatrix} I_1 \\ I_2 \\ I_w \end{bmatrix} \quad (1)$$

By rearranging this determinant eqation and eliminating the currents I_1 and I_2 flowing through the current injecting probe and the current receiving probe, we can derive the load impedance Z_L as follows:

$$Z_L = K\left(\frac{V_{p1}}{V_{p2}}\right) - Z_{setup} \quad (2)$$

where K and Z_{setup} are the calibration coefficients that are functions of M_1, M_2, Z_{p1}, Z_{p2}, L_w, r_w, and represent the characteristics of the measurement system. Also, the voltage ratio $\frac{V_{p1}}{V_{p2}}$ is expressed as follows using S_{11} and S_{21} measured by the network analyzer:

$$\frac{V_{p1}}{V_{p2}} = \frac{S_{11}+1}{S_{21}}. \quad (3)$$

The calibration coefficients K and Z_{setup} can be obtained by performing calibration according to the following procedure before measurement starts.

- Measure S_{11} and S_{21} when short-circuiting the end of the closed loop with the network analyzer and obtain the voltage ratio $\frac{V_{p1}}{V_{p2}}$ by (3).
- Measure S_{11} and S_{21} when the network termination of the closed loop is known resistor R_{std} and obtain the voltage ratio $\frac{V_{p1}}{V_{p2}}$ by (3).
- Calculate the calibration coefficients K and Z_{setup} by the following equation:

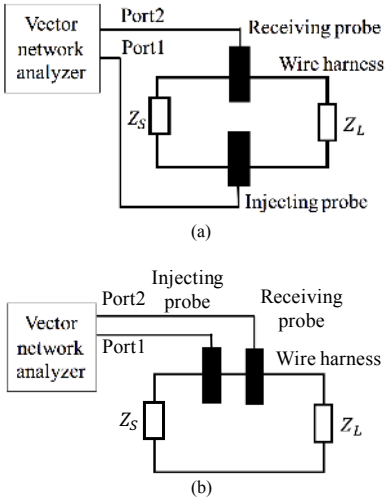

Fig. 3. Non-contact measurement system of load impedance when regarding the wire harness as a transmission line. (a) Two parallel wires. (b) A wire above a ground plane by considering the wire's image with respect to the ground plane as the return wire.

$$K = \frac{Z_L|_{Z_L=R_{std}}}{\left.\frac{V_{p1}}{V_{p2}}\right|_{Z_L=R_{std}} - \left.\frac{V_{p1}}{V_{p2}}\right|_{Z_L=short}} \quad (4)$$

$$Z_{setup} = K\left.\frac{V_{p1}}{V_{p2}}\right|_{Z_L=short} \quad (5)$$

After obtaining the calibration coefficients K and Z_{setup} of the measurement system, we can measure the S_{11} and S_{21} and substitute them into (2) and (3) to obtain the impedance of the unknown load.

However, in this measurement method, the length of the wire harness should be sufficiently short as compared with the wavelength, and therefore it is a precondition that the impedance viewed from the current injecting probe and the current receiving probe to the load side is equal to the load impedance. As a result, when the frequency becomes so high that the length of the wire harness can not be ignored, the measurement error becomes conspicuous, so that it can only be applied to 20∼30 MHz at present.

III. Extension to High Frequency by Application of Transmission Line Concept

In order to expand this measurement method to higher frequencies, we regard the two wires from the current injecting probe and the current receiving probe to the load as a transmission line. Figs. 3 and 4 show the measurement system and equivalent circuit, respectively, here we consider two cases. One case is a component connected at the end of two parallel wires, and the other case is a component connected at the end of a wire above a ground plane. We will show that the formula for the load impedance is in the same form as (2).

A. Two Parallel Wires

Under the condition that the spatial interval between the parallel wiring harnesses is sufficiently small compared with

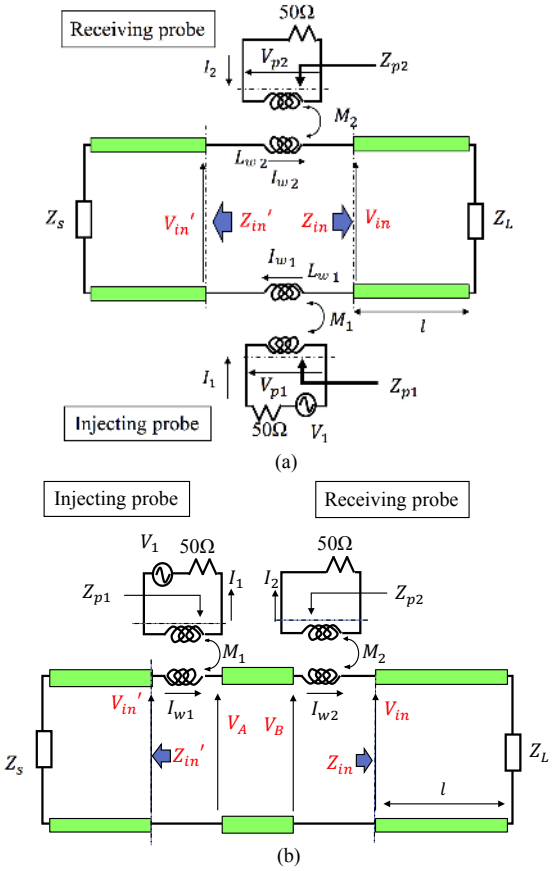

Fig. 4. Equivalent circuit of non-contact measurement system of load impedance when regarding the wire harness as a transmission line. (a) Two parallel wires. (b) A wire above a ground plane.

the wavelength with respect to the upper limit frequency (100 MHz), a current with opposite phase to the current applied from the current injecting probe will flow at the receiving probe location. This is actually a quasi-TEM propagation mode assumption. In order to confirm this assumption, we analyzed the current phase difference at the current injecting probe and the receiving probe using an electromagnetic field simulator. As a result, we confirmed the assumption valid as long as the interval between the two wire harnesses is smaller than 1/10-wavelength.

For the equivalent circuit of Fig. 4(a), the voltage drop equations in the three loops can be written as:

$$V_1 = (50 + Z_{p1})I_1 - j\omega M_1 I_{w1} \tag{6}$$

$$0 = (50 + Z_{p2})I_2 + j\omega M_2 I_{w2} \tag{7}$$

$$\begin{aligned} V_{in} - V_{in}' &= -j\omega M_1 I_1 + j\omega M_2 I_2 \\ &\quad + j\omega L w_{w1} I_{w1} + j\omega L_{w2} I_{w2} \end{aligned} \tag{8}$$

Also, the following equation holds.

$$V_{in} = Z_{in} I_{w2} \tag{9}$$

$$V_{in}' = -Z_{in}' I_{w1} \tag{10}$$

Then by eliminating I_1, I_2, V_{in} and V_{in}' we obtain

$$\begin{aligned} &j\omega M_1 \frac{V_1}{50 + Z_{p1}} - Z_{setup1} I_{w1} \\ &= Z_{in} I_{w2} + Z_{in}' I_{w1} + Z_{setup2} I_{w2} \end{aligned} \tag{11}$$

where Z_{setup1} and Z_{setup2} are functions of M_1, M_2, L_{w1}, L_{w2}, Z_{p1} and Z_{p2}. Since the relationship between the currents I_{w1}, I_{w2} and the voltages V_{p1}, V_{p2} at the probe location on the wire harness can be expressed using the transfer impedance Z_{T1} and Z_{T2} of the probe, we have

$$I_{w1} = \frac{V_{p1}}{Z_{T1}} \tag{12}$$

$$I_{w2} = \frac{V_{p2}}{Z_{T2}} \tag{13}$$

$$V_1 = \frac{50 + Z_{p1}}{Z_{p1}} V_{p1} \tag{14}$$

Substitute (12) - (14) into (11) we finally have

$$Z_{in} = K\left(\frac{V_{p1}}{V_{p2}}\right) - Z_{setup} \tag{15}$$

where K and Z_{setup} are different from those in (2) and are given in (33) and (34) in Appendix, respectively.

Therefore, even if we regard the wire harness as a transmission line, its influence can still be included in the calibration coefficients and an equation similar to (2) in Section II can still be derived.

B. A Wire above a Ground Plane

When the wire harness is above a ground plane, we still can regard the structure as a two-wire transmission line by considering the wire's image with respect to the ground plane. In this case we can not arrange the two probes in the form as in Fig. 3(a). So we have to arrange the two probes as shown in Fig. 3(b) with the corresponding equivalent circuit in Fig. 4(b).

Again, (6) and (7) hold for this measurement system. But instead of (8), we have

$$V_{in}' - V_A = -j\omega M_1 I_1 + j\omega L_{w1} I_{w1} \tag{16}$$

$$V_B - V_{in} = j\omega M_2 I_1 + j\omega L_{w2} I_{w2} \tag{17}$$

By summing up (16) and (17) and rearranging it using (9) and (10), we obtain

$$\begin{aligned} V_B - V_A &= j\omega M_2 I_2 + (j\omega L_{w2} + Z_{in}) I_{w2} \\ &\quad - j\omega M_1 I_1 + (j\omega L_{w1} + Z_{in}') I_{w1} \end{aligned} \tag{18}$$

On the other hand, for the wire segment between the two probes, we can express it using F matrix as

$$\begin{bmatrix} V_A \\ I_{w1} \end{bmatrix} = \begin{bmatrix} A & B \\ C & D \end{bmatrix} \begin{bmatrix} V_B \\ I_{w2} \end{bmatrix}. \tag{19}$$

From (16) - (19) with the aid of (12) - (14), we can obtain V_{in} and I_{w2} after some complicated operations, and then derive Z_{in} still in the following form

$$Z_{in} = K\left(\frac{V_{p1}}{V_{p2}}\right) - Z_{setup} \tag{20}$$

where K and Z_{setup} are different from those in (15) and are given in (35) and (36) in Appendix, respectively.

C. Application of Transmission Line Concept

In the conventional method described in Section II, the impedance at the measurement point of S parameter is set to the end load impedance Z_L. However, it should be the input impedance Z_{in} as seen from the measurement position in the case of two parallel wires and the case of a wire above a ground plane in Fig. 4. Between Z_{in} and Z_L, the following equation holds according to the transmission line theory [6].

$$Z_{in} = Z_0 \frac{Z_L + Z_0 \tanh(\gamma l)}{Z_0 + Z_L \tanh(\gamma l)} \tag{21}$$

where Z_0 and $\gamma = \alpha + j\beta$ are the characteristic impedance and propagation constant (α: attenuation constant; β: phase constant) of the transmission line structure, respectively, and l is the length of the wire from the measurement position to the load. In view of that the considered frequencies are lower than 100 MHz, the propagation loss is small for a wire harness shorter than the wavelength, so that it is reasonable to only consider the phase constant β, i.e., $\gamma = j\beta$. For deriving the calibration coefficients K and Z_{setup}, it is necessary to regard the part of the wire harness as a transmission line, and set the end load as short-circuited or a standard resistance R_{std}. Then we can have

$$Z_{in}|_{Z_L=short} = K \left(\frac{V_{p1}}{V_{p2}}\right)\Big|_{Z_L=short} - Z_{setup} \tag{22}$$

$$Z_{in}|_{Z_L=R_{std}} = K \left(\frac{V_{p1}}{V_{p2}}\right)\Big|_{Z_L=R_{std}} - Z_{setup} \tag{23}$$

From (23) and (24) we can obtain the calibration coefficients K and Z_{setup} as follows

$$K = \frac{Z_{in}|_{Z_L=R_{std}} - Z_{in}|_{Z_L=short}}{\frac{V_{p1}}{V_{p2}}\Big|_{Z_L=R_{std}} - \frac{V_{p1}}{V_{p2}}\Big|_{Z_L=short}} \tag{24}$$

$$Z_{setup} = K \left.\frac{V_{p1}}{V_{p2}}\right|_{Z_L=short} - Z_{in}|_{Z_L=short} \tag{25}$$

Then the unknown load impedance at the end of the wire harness can be obtained by first obtaining $Z_{in}|_{Z_L=unknown}$ by (15) or (20) using the calibration coefficients K and Z_{setup}, and then by the following equation

$$Z_L = Z_0 \frac{Z_{in}|_{Z_L=unknown} - jZ_0 \tan(\beta l)}{Z_0 - jZ_{in}|_{Z_L=unknown} \tan(\beta l)}. \tag{26}$$

IV. Estimation Method of Characteristic Impedance and Propagation Speed

The measurement system composed of the wire harness of Fig. 3 basically has a structure of parallel lines. We therefore need to estimate the characteristic impedance Z_0 and the phase constant β of the wire harness when viewing the load side as a transmission line from the position of the measuring probe. They can be estimated at the same time of determining the calibration coefficients K and Z_{setup} by using three known loads: short-circuited terminal load, R_{std1} and R_{std2}.

First, by measuring S_{11} and S_{21} when terminating loads are short-circuited, R_{std1} and R_{std2}, respectively, the voltage ratio $\left.\frac{V_{p1}}{V_{p2}}\right|_{short}$, $\left.\frac{V_{p1}}{V_{p2}}\right|_{R_{std1}}$ and $\left.\frac{V_{p1}}{V_{p2}}\right|_{R_{std2}}$ are obtained. Next, the relation between the input impedance Z_{in} and the calibration coefficients K and Z_{setup} at the measurement position are shown below

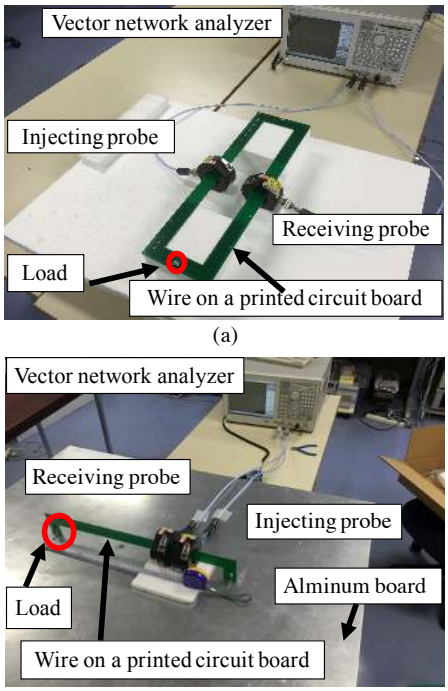

Fig. 5. View of verification experiment. (a) Two parallel wires. (b) A wire above a ground plane.

$$Z_{in}|_{short} = K \left.\frac{V_{p1}}{V_{p2}}\right|_{short} - Z_{setup} \tag{27}$$

$$Z_{in}|_{R_{std1}} = K \left.\frac{V_{p1}}{V_{p2}}\right|_{R_{std1}} - Z_{setup} \tag{28}$$

$$Z_{in}|_{R_{std2}} = K \left.\frac{V_{p1}}{V_{p2}}\right|_{R_{std2}} - Z_{setup} \tag{29}$$

Solving (27) and (28) for K and Z_{setup} gives

$$K = \frac{Z_{in}|_{short} - Z_{in}|_{R_{std1}}}{\left.\frac{V_{p1}}{V_{p2}}\right|_{short} - \left.\frac{V_{p1}}{V_{p2}}\right|_{R_{std1}}} \tag{30}$$

$$Z_{setup} = K \left.\frac{V_{p1}}{V_{p2}}\right|_{short} - Z_{in}|_{short} \tag{31}$$

Substituting (30) and (31) into (29) yields the following equation

$$\frac{Z_{in}|_{R_{std2}} - Z_{in}|_{short}}{Z_{in}|_{short} - Z_{in}|_{R_{std1}}} = \frac{\left.\frac{V_{p1}}{V_{p2}}\right|_{R_{std2}} - \left.\frac{V_{p1}}{V_{p2}}\right|_{short}}{\left.\frac{V_{p1}}{V_{p2}}\right|_{short} - \left.\frac{V_{p1}}{V_{p2}}\right|_{R_{std1}}} \tag{32}$$

In (32), the left side is functions of the characteristic impedance Z_0 and the phase constant β, and the right side can be obtained from the measured S_{11} and S_{21}. Since Z_0 and $\omega/\beta = v$ (ω : angular frequency; v: propagation speed)

TABLE I
EXPERIMENTAL PARAMETERS

Frequency range	300 kHz - 100 MHz
Network analyzer	Agilent E5071B
Current probe	ETS-91550-1
Length of wire harness	450 mm (l = 350, 400 mm)
Radius of wire harness	0.5 mm
Interval between wire harnesses	110 mm (Two parallel wires)
Height of wire harnesses	55 mm (A wire above a ground plane)
Calibration resistor	Short, 1 kΩ, 2 kΩ
Load resistor to be measured	3 kΩ, 10 kΩ
Load capacitor to be measured	470 pF, 1000 pF

TABLE II
ESTIMATED PARAMETERS OF TRANSMISSION LINE

	Estimated	Simulated
Z_0	498.0 Ω	487.6 Ω
v	2.8x10^8 m/S	2.0x10^8 m/S

are constants irrelevant to frequency, we can estimate them using the least squares method by taking them as unknowns in (32). The fitting tool in Matlab is useful to this purpose.

V. MEASUREMENT PROCEDURE

The measurement procedure is summarized as follows:

- Measure S_{11} and S_{21} when the terminal loads are shorted, R_{std1} and R_{std2}, respectively, and calculate $\frac{V_{p1}}{V_{p2}}$ from (3) to obtain the right side of (32). At this time, accurate R_{std1} and R_{std2} are measured in advance using an impedance analyzer and a special jig.
- Apply the least squares method to (32) to estimate the characteristic impedance Z_0 and propagation speed v.
- Derive the calibration coefficients K and Z_{setup} from (30) and (31) using Z_{in} calculated from (21) when the terminal loads are short-circuited, R_{std1} and R_{std2}, respectively.
- Measure S_{11} and S_{21} when the load Z_L to be measured is connected to the end of wire harness, and obtain $Z_{in}|_{Z_L=unknown}$ from (15) or (20).
- Calculate the load impedance Z_L from (26).

VI. EXPERIMENTAL VERIFICATION

A. Verification of Measurement Accuracy

The validity of the measurement method was experimentally verified for both the case of two parallel wires and the case of a wire above a ground plane. Table 1 shows the specifications of the verification experiment, and Fig. 5 shows the experimental view. For selecting the calibration resistor value, it is desirable to use a short circuit terminal and an open terminal. However, it is difficult to realize the open termination, and the accuracy of a resistor with a large resistance value is generally not good either. Therefore, in this study, besides the short circuit, the resistors with 1 kΩ and 2 kΩ, that are not only larger than the load assumed for automobile parts but also have sufficiently high accuracy, were chosen for calibration. In fact, we have experimentally confirmed that the calibration results were the same when we changed the calibration resistor values between 1 kΩ and 10 kΩ. As long as the calibration resistors were larger than several kΩs, no obvious difference was observed in the measured load impedance.

Table 2 shows the characteristic impedance Z_0 and propagation speed v of the wire harness estimated when R_{std1} = 1 kΩ and R_{std2} = 2 kΩ. The estimated values are the fitting results for (32), while the simulated values are obtained for a simplified model of the measurement system using an electromagnetic field simulator (2D Extractor). Two reasons can be considered for the differences between the estimated and simulated values. One reason is the fitting error in Eq. (32). The other reason is due to simplification of modeling, because the injecting and receiving probes were not taken into consideration. In fact, both of them contributed to the differences in Table II. In other words, the estimated parameter Z_0 and v actually contains the influences of probes and others that are difficult to be obtained by a simple two-dimensional simulation or theoretical formula.

Fig. 6 shows the absolute values of the measured load impedance in the case of two parallel wires where the position of the probes was 400 mm from the terminal load, and Fig. 7 shows the absolute values of the measured impedance in the case of a wire above a ground plane where the position of the probes was 350 mm from the terminal load. In both case the left side of the measurement system was shorted, i.e., Z_s = 0, but it was not necessary to know its actual value. For comparison, the conventional method without applying the transmission line theory and the actual values measured by an impedance analyzer are also shown.

From Figs. 6 and 7, it can be seen that the discrepancy from the actual value becomes conspicuous when the frequency is 30 MHz or more in the conventional method. However, in the proposed method, they agree with an error within 10% up to 100 MHz. Moreover, the resonance frequency which was difficult to confirm by the conventional method in the measurement of capacitive load could be confirmed in the proposed measurement method. It should be mentioned that, although the wires used in the experiment were not sufficiently long with respect to typical automotive harness, they indeed demonstrated the insufficiency of the conventional method. Without employing the transmission line theory as proposed, the validity of the measurement method is limited to below 20∼30 MHz. While employing the proposed method, the validity of measurement has been extended to up to 100 MHz. So the experimental structure in this study is useful to validate the proposed extension, and the principle is also same when applying the method to longer wires.

Incidentally, the reason of the errors between the measurement results and the actual values may be due to an error of the characteristic impedance and propagation speed of the wire harness, or the influence of a parasitic component of the wire portion at the load. In order to clarify the influence of estimation error of the characteristic impedance Z_0 and propagation speed v on load impedance measurement, we conducted an error analysis. For the case of two parallel wires with a resistor of 3 kΩ, we assumed a ±10% difference from the actual values of Z_0 and v, and used them to derive the

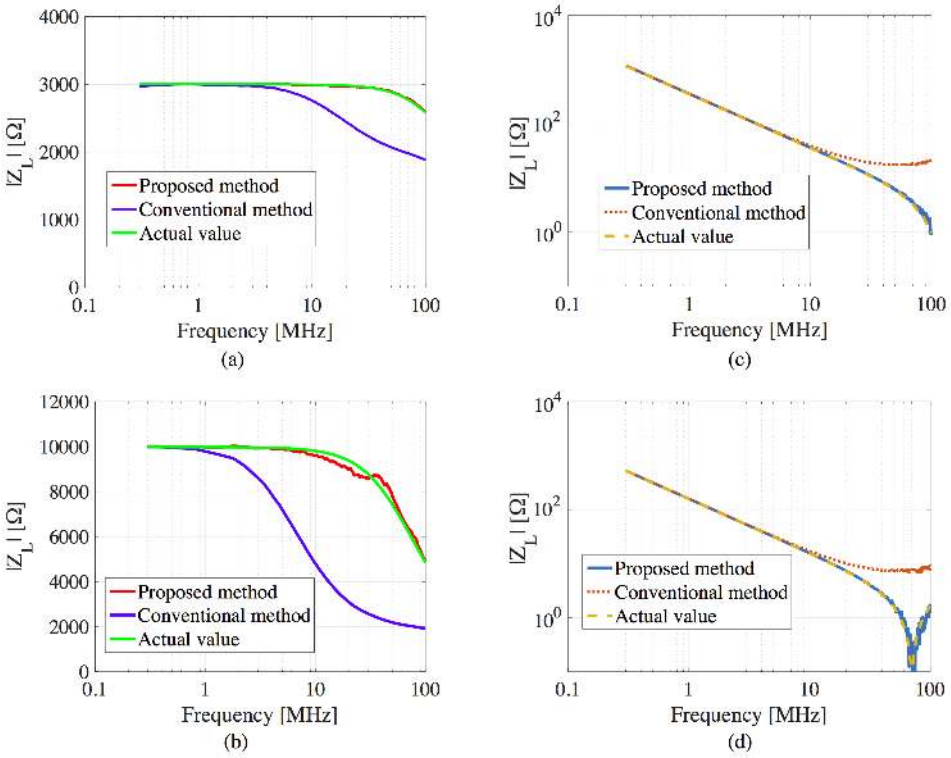

Fig. 6. Measured absolute values of impedance in the case of two parallel wires (l = 400 mm, Z_s = 0). (a) Load resistor = 3 kΩ. (b) Load resistor = 10 kΩ. (c) Load capacitor = 470 pF. (d) Load capacitor = 1000 pF.

TABLE III
INFLUENCE OF Z_0 AND v ON MEASUREMENT ERROR OF LOAD IMPEDANCE

Relative error	1 MHz	10 MHz	50 MHz	100 MHz
Z_0: +10%	-0.2%	-0.7%	-2.9%	-2.3%
Z_0: -10%	-0.2%	0.2%	3.8%	5.0%
v: +10%	0.0%	0.0%	6.9%	15.7%
v: -10%	0.0%	-1.0 %	-8.1%	-11.6%

load impedance. Table III summarizes the measurement result. It can be seen that the estimation error of load impedance is more sensitive at higher frequencies and for propagation speed v. An estimation error of 10% on Z_0 or v may yield a measurement error on load impedance up to 0.7% at 10 MHz and 15.7% at 100 MHz.

B. Effect of Loading at the Left Side

In the derivation of the estimation formulas, we mentioned that the calibration coefficients include the influence of the left side load of the transmission line, which was also experimentally verified. The measurement was carried out when a load ($Z_s = 51\Omega$) was attached to the left side of the loop which had been short-circuited so far. But in applying the measurement method, we assumed it as unknown. The measurement result is shown in Fig. 8. As can be seen, the load impedance on the right side of the circuit loop was correctly measured even when a load was attached to the left side.

C. Application to Motors under Operation

As an actual example of applications, we applied the proposed method to measure the load impedance for two commercial motors (named as Motor A and B) under operation. The measurement setup is the same as the case of a wire above a ground plane. The right side was connected to the motors, and the left side was connected to a battery. The length of wire was one meter. The battery had a switch for power on and off to make the motors operate or not. When calibrating the measurement setup, we employed a resistor of 51 Ω instead of the short termination because shortening the motors is dangerous for battery. The other two calibration resistors were still 1 kΩ and 2 $k\Omega$. Fig. 9 shows the measured absolute values of load impedance when the two motors operated or not, respectively. It is obvious that the motor impedance differed from the power-off condition when they were under operation conditions. The load impedance for the motor in Fig. 9(a) was inductive at frequencies below 7 MHz, and then became conductive at frequencies above 7 MHz. When the power was on, the load impedance varied within a range at some frequencies, and a new peak frequency was observed around 60 MHz. In Fig. 9(b), the motor's load impedance exhibits a capacitive characteristic at low frequencies and then an inductive characteristic above tens of MHz. This feature was explainable from the structure of the motor where two capacitors were connected between each output terminal and the motor housing. But a shift of resonance frequency from 10 MHz to 18 MHz was observed when the power was on.

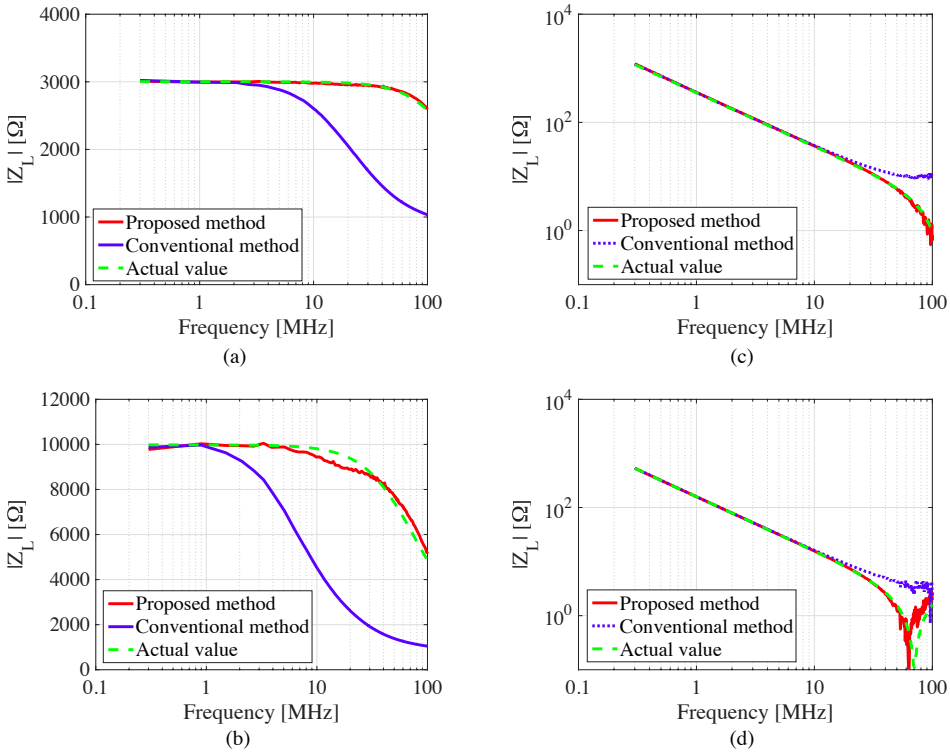

Fig. 7. Measured absolute values of impedance in the case of a wire above a ground plane (l = 350 mm, Z_s = 0). (a) Load resistor = 3 kΩ. (b) Load resistor = 10 kΩ. (c) Load capacitor = 470 pF. (d) Load capacitor = 1000 pF.

These results suggest that just measuring the load impedance under the power-off condition is insufficient, and a non-contact measurement method as described in this study is essential.

However, under the power-on condition, high frequency noises from the motors may also flow along the wire harness and thus affect the accuracy of measurement. So the injecting current from the probe should be as large as possible in order to make the influence of noise currents insignificant. For Fig. 9, in view of the good reproducibility on the measured impedance for the two motors, the influence of high frequency noises seemed not noticeable, because a time-varying motor noise should yield a low reproducibility of impedance measurement.

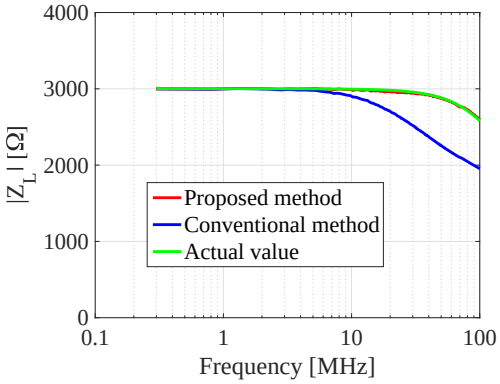

Fig. 8. Measured absolute values of impedance of a resistive load when an unknown load ($Z_s \neq 0$) was attached to the left side.

VII. Conclusions

Non-contact measurement of the impedance of load at the end of wire harness is important in predicting emission and immunity characteristics. However, the conventional non-contact impedance measurement method using the network analyzer and current probes is limited to 20∼30 MHz even if an error of 10% is allowed. In this study, we have proposed to apply the transmission line theory to the conventional method for extending it to higher frequencies. We have also proposed a method to estimate the actual characteristic impedance and phase constant for applying in our proposed non-contact impedance measurement. As a result of experiments, the load impedance up to 100 MHz has been measured with an error within 10% for both resistive loads and capacitive loads. The measurement results for two motors under operation condition have also demonstrated the importance of non-contact impedance measurement.

A future subject is to quantitatively study the possible influence of high frequency noise currents from an active load, and extend the measurement method to higher frequencies.

References

[1] B. Garry and R. Nelson, “Effect of impedance and frequency variation on insertion loss for a typical power line filter”, Proc. IEEE EMC Symp., pp.691-695, 1998.

[2] D. Zhang, D.Y. Chen, M.J. Nave, and D. Dable, “Measurement of noise source impedance of off-line converters”, IEEE Trans. Power Electron., vol.15, no.5, pp.820-825, Sept. 2000.

[3] K.Y. See and J. Deng, “Measurement of noise source impedance of SMPS using a two probes approach”, IEEE Trans. Power Electron., vol.19, no.3, pp.862-868, May 2004.

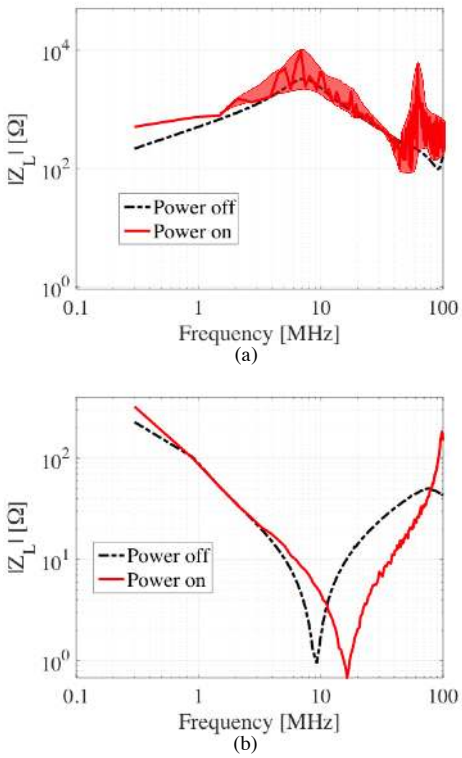

Fig. 9. Measured absolute values of load impedance of two motors. (a) Motor A. (b) Motor B.

[4] V. Tarateeraseth, B. Hu, K.Y. See, and F.G. Canavero, "Accurate extraction of noise source impedance of an SMPS under operating condition", IEEE Trans. Power Electron., vol.25, no.1, pp.111-117, Jan. 2010.
[5] F. Grassi, F. Marliani and S.A. Pignari, "Circuit modeling of injection probes for bulk current injection", IEEE Trans. Electromagn. Compat., vol.49, no.3, pp.563-576, Aug. 2007.
[6] T. Sato, Transmission Circuit (in Japanese), CORONA Publishing, 1963, pp. 328-340.

APPENDIX

Two parallel wires::

$$K = \frac{j\omega M_1}{50+Z_{p1}} Z_{T2} - \left(\frac{\omega^2 M_1^2}{50+Z_{p1}} + j\omega L_{w1} + Z'_{in}\right)\frac{Z_{T2}}{Z_{T1}} \quad (33)$$

$$Z_{setup} = \frac{\omega^2 M_2^2}{50+Z_{p2}} + j\omega L_{w2} \quad (34)$$

A wire above a ground plane:

$$K = \frac{j\omega M_1}{Z_{p1}} Z_{T2} - \left(\frac{\omega^2 M_1^2}{50+Z_{p1}} + j\omega L_{w1} + Z'_{in} + \frac{A-1}{C}\right)\frac{Z_{T2}}{Z_{T1}} \quad (35)$$

$$Z_{setup} = \frac{\omega^2 M_2^2}{50+Z_{p2}} + j\omega L_{w2} + B + \frac{D-AD}{C} \quad (36)$$

PLACE PHOTO HERE

Tomohiro Yoshikawa received the B.E. degree in electrical and electronic engineering from, Nagoya Institute of Technology, Nagoya, Japan, in 2016. He is currently engaged in research on non-contact measurement method of load impedance towards his master degree of engineering also at Nagoya Institute of Technology.

PLACE PHOTO HERE

Jianqing Wang received the B.E. degree in electronic engineering from the Beijing Institute of Technology, Beijing, China, in 1984, and the M.E. and D.E. degrees in electrical and communication engineering from Tohoku University, Sendai, Japan, in 1988 and 1991, respectively. He was a Research Associate at Tohoku University and a Senior Engineer at Sophia Systems Co., Ltd., prior to joining the Nagoya Institute of Technology, Nagoya, Japan, in 1997, where he has been a Professor since 2005. His research interests include biomedical communications and electromagnetic compatibility.

PLACE PHOTO HERE

Yasunori Oguri received the B.E. and M.E. degrees in information and communication engineering from the University of Electro-Communications, Tokyo, Japan, in 2006 and 2008, respectively. In 2008, he joined DENSO CORPORATION. He is currently engaged in the development of EMC design technology for in-vehicle electronic equipment.

PLACE PHOTO HERE

Makoto Tanaka received the B.E. degree in electronic information engineering from Yokohama National University, Yokohama, Japan, in 1997. In 1997, he joined DENSO CORPORATION. He is currently engaged in the development of EMC design technology for in-vehicle electronic equipment.

PLACE PHOTO HERE

Michihira Iida received the B.E. degree in electrical engineering from Nihon University, Japan, in 1981, and the Dr. Eng. degree in Computer Science and Engineering from Nagoya Institute of Technology, Japan, in 2013. In 1981, he joined Shin Nihon Denki, where he was engaged in the development, design and evaluation of parts for CRT display. In July 1986, he joined DENSO CORPORATION. Since then he has engaged in developing new products for automotive electronic devices. He is currently engaged in radio wave certification acquisition and EMC evaluation of in-vehicle electronic equipment.